World Academy of Science, Engineering and Technology
International Journal of Energy and Power Engineering
Vol:12, No:2, 2018

# Comparative Study of Sub-Critical and Supercritical ORC Applications for Exhaust Waste Heat Recovery

Buket Boz, Alvaro Diez

International Science Index, Energy and Power Engineering Vol:12, No:2, 2018 waset.org/Publication/10008559

***Abstract*—**Waste heat recovery by means of Organic Rankine Cycle is a promising technology for the recovery of engine exhaust heat. However, it is complex to find out the optimum cycle conditions with appropriate working fluids to match exhaust gas waste heat due to its high temperature. Hence, this paper focuses on comparing sub-critical and supercritical ORC conditions with eight working fluids on a combined diesel engine-ORC system. The model employs two ORC designs, Regenerative-ORC and Pre-Heating-Regenerative-ORC respectively. The thermodynamic calculations rely on the first and second law of thermodynamics, thermal efficiency and exergy destruction factors are the fundamental parameters evaluated. Additionally, in this study, environmental and safety, GWP (Global Warming Potential) and ODP (Ozone Depletion Potential), characteristic of the refrigerants are taken into consideration as evaluation criteria to define the optimal ORC configuration and conditions. Consequently, the studys outcomes reveal that supercritical ORCs with alkane and siloxane are more suitable for high temperature exhaust waste heat recovery in contrast to sub-critical conditions.

***Keywords*—**Internal combustion engine, organic rankine cycle, waste heat recovery, working fluids.

## I. Introduction

FROM a sustainability standpoint, efficient energy conversion processes are one of main concerns for the $21^{st}$ century. The implementation of new renewable energy systems is essential to increase sustainability and reduce greenhouse gases. On the other hand, internal combustion engines (ICE) are still the primary power source for transportation and small-scale power generation and the ascendancy of ICE will not be changed in the near future. Nevertheless, over half of the energy contained in the fuel cannot be converted into useful work and it is discharged to the ambient as waste heat through exhaust or cooling systems. The thermal efficiency of a standard ICE is less than 45%, Hence, waste heat recovery (WHR) applications can reduce greenhouse gas emissions and improve the efficiency of the engine without adding fuel. Several methods have been explored among which Organic Rankine Cycle ORC was drawn the attention for its high efficiency and excellent adaptability [1].

A substantial amount of research on waste heat recovery applications focus on ORC [2]-[5]. ORCs are considered as the most suitable method for WHR due to its simplicity, performance and cost [6], [7].

Buket Boz is with the Department of Energy Engineering, Izmir Institute of Technology, Turkey (e-mail: buketboz90@gmail.com).
Alvaro Diez is with the Izmir Institute of Technology, Turkey.

Vaja et al. [8] employed three ORC configurations with three working fluids on a stationary diesel engine. The highest increase of the efficiency was obtained from the regenerated and preheated cycles with values close to 12.5% with the application of benzene. Meanwhile, R11 performed slightly lower but close to benzene application while solely preheating configuration was employed and resulted with the value of 11%. In the work of Uusitalo et al. [4], an ORC system was investigated looking into the effect of different working fluids namely, toluene, n-pentane, R-245fa and cyclohexane. Toluene and cyclohexane gave the highest power outputs in contrast to the other two selected working fluids. The maximum power increase of 11.4% was obtained from the exhaust gas of a large scale gas-fired engine. The increment from the charge air heat was only 2.4%.

In the study of Kulkarni et al., a dual ORC was suggested for a heavy duty ICE with working fluids as R245fa and R236fa for the high temperature (HT) and low temperature (LT) loops respectively. The heat from both exhaust gases was utilised in the HT loop, engine block and the residual heat from HT loop was applied in the LT loop. As a consequence, the overall thermal efficiency of the system was risen up to 10% [5].

The choice of working fluid significantly influences the achievable performance. Peris et al. [9] investigated six ORC configurations with ten non-flammable working fluids evaluated in terms of efficiency, safety, costs and environment. They showed that the single Regenerative ORC with R236fa as the working fluid and the Reheat Regenerative ORC offered the highest efficiencies. The net efficiency was calculated to be 6.5%, the ICE efficiency rose up to 4.6%. An exergy analysis was applied to determine the working fluid for supercritical and sub-critical conditions and revealed a possible improvement of the net power output by Schuster et al. [10]. The selection of the working fluid for ORC applications relies on several criteria such as thermodynamic properties, environmental properties, etc.. In the work of Glover et al. the general increment trend on the cycle efficiency was related to the higher critical temperature of the organic fluids [11].

In terms of vehicle applications, BMW introduced a dual-loop ORC, which uses water and ethanol as working fluids for high and low temperature cycles [12]. Additionally, Agudelo et al. investigated the potential of exhaust gases of a light duty diesel car under European driving cycle conditions and stated that the fuel consumption was decreased between 8-19% [13]. In accordance with International Energy Agency, the importance of implementation of WHR on vehicles is

International Science Index, Energy and Power Engineering Vol:12, No:2, 2018 waset.org/Publication/10008559

directly associated with reduction of $CO_2$ emissions [14].

More recently, the focus on supercritical ORC employments has been increased due to its higher thermodynamic performance. The fundamental aspect of supercritical ORC over a sub-critical is a better match between the heat source's cooling curve and the refrigarent's heating curve [15]. For instance, Glover et al. simulated supercritical ORC with several working fluids and concluded that the WHR-ORC efficiencies from 5% to 23% could be achieved [16]. Ho Teng et al. also presented a detailed supercritical ORC application for heavy duty diesel engines. Ho Teng summaried the studies in two paper and revealed that up to 20% increment in engine power could be achieved by DE-ORC system [17], [18].

Although an extensive literature about ORC is available, this study presents an investigation of ORC, in which not only thermal efficiency but the exergy loss, the second law efficiency and exergy destruction factor are evaluated. Furthermore, two configurations are presented RORC and PRORC covered under sub-critical and supercritical conditions. In addition, 8 working fluids representing five chemical classes are employed, thus providing an in-depth analysis of these configurations.

## II. Methodology

In the present study, sub-critical and supercritical ORCs are employed to comprehend the differences between two applications with respect to the pressure of the cycle and the turbine inlet temperature. Through the analysis, Regenerative and Pre-Heating-Regenerative ORC are designed to acquire the most applicable configurations with the proper working fluid. The first set-up is thermally powered by only exhaust gases, whilst, the PRORC uses both exhaust gases and the engine cooling water as the heat source. The mathematical model of ORCs comprises a set of energy balance equations, which are applied through the first and second law of thermodynamics. Several assumptions are made to conceive the relevant ORC systems:

- The pressure losses in the heat exchangers and pipes are neglected for the study.
- State-1, the condenser temperature is set at $35°C$ and the working fluid is considered as saturated liquid.
- The pump and turbine's isentropic efficiencies are taken 75% and 80% respectively [8].
- To prevent the liquid droplets formation on the turbine blades at the end of the expansion process, dry expansion is assumed for the eight organic fluids.
- For the sub-critical applications, the pinch point approach is applied to calculate the heat transfer between exhaust gas and working fluid. For the evaporator, $\Delta T_{pp}$ is set to 30 K for both designs. ($\Delta T_{pp}$ = 30 K, Pinch point temperature difference). In addition, the position of the pinch point is set to the starting point of the vaporisation.
- For the regenerative case, $\Delta T_{approach}$ = 15 K $\Delta T_{approach}$ (Temperature difference between the fluids in the heat exchanger) is taken in order to satisfy the demand of the heat exchanger.
- The pressure ratio between the evaporator and the critical pressure of the working fluid is fixed to 90% for sub-critical ORCs (Analysis on the election of evaporator's pressure is presented in Section III-A). Meanwhile, the evaporator pressure is set to 7 MPa for the supercritical applications. The pressure limit is fixed taken into consideration the commercial application of ORC turbines [19].

In Table I, the main features of the diesel engine are indicated. The equivalence ratio at full load was 0.45. Under the assumption of complete combustion with an excess of air, $c_p$ value was acquired for the engine exhaust gas.

TABLE I
Engine's Parameters

| Features | Stationary Diesel Engine |
|---|---|
| Power [kW] | 1320 |
| Volume [L] | 45.8 |
| Speed / Frequency [rpm/Hz] | 1500/50 |
| $T_{exh,out}$ [$°C$] | 455 |
| $\dot{m}_{exh}$ [kg/s] | 2.595 |
| $c_{p,exh}$[kJ/kgK] | 1.085 |

The mathematical model, used to calculate the thermodynamic states, is explained in detail in Appendix.

### A. Working Fluid Selection

The working fluid plays a crucial role in ORC applications and many investigations have focused on finding suitable fluids for this kind of application [20], [21]. While, the candidate organic fluids are selecting for the process, the key aspects should be taken into consideration are environmental, thermodynamic properties and safety legislations.
Two primary points for selection of working fluids:

- In terms of environmental concerns, ozone depletion potential (ODP) and global warming potential (GWP) values of the organic fluids and their compatibility with the EU legislations have taken into account. In addition, the American Society of Heating, Refrigerating and Air-Conditioning Engineers' (ASHRAE) standards are deliberated over working fluids in terms of safety class.
- The critical pressure and temperature of the working fluids should compromise the limits of the cycle conditions.

## III. Results and Discussion

### A. Sub-Critical Pressure Ratio Selection

Fig. 1 shows the thermal efficiency outcomes with respect to seven pressure ratios for the sub-critical ORC. As expected the thermal efficiency of all working fluids increased with the increase of evaporator's pressure. This was due to the increase of Turbine inlet temperature that led to the total net work output increased. As all working fluids behaved in a similar manner, a single condition of the sub-critical ORC cycles was selected for the comparison with the supercritical conditions. Hence the evaporator pressure was set to 90% of the critical pressure of the each working fluids. Table III shows the evaporator pressure and Turbine inlet temperature for each working fluids under sub-critical conditions used in the comparison with the supercritical cycles.

TABLE II
THE CANDIDATE WORKING FLUIDS

| Fluid | Chem.Class | Slope | $P_{crit}$ [kPa] | $T_{crit}$ [K] | ODP | GWP | Safety Class |
|---|---|---|---|---|---|---|---|
| R-134a | HFC | Isentopic | 4059.2 | 374.2 | 0 | 1430 | B1 |
| R-245fa | HFC | Isentropic | 3651.4 | 427.2 | 0 | 1030 | B1 |
| R-1234yf | HFO | Dry | 3382.1 | 367.8 | 0 | $< 4.4$ | A2Lr |
| R-1233zd-E | HFO | Dry | 3570.1 | 438.7 | 0.00034 | 7 | A1 |
| R-1234ze-E | HFO | Dry | 3634.6 | 382.5 | 0 | 6 | A2L |
| Cyclohexane | Alkane | Dry | 4080.1 | 553.6 | 0 | very low [22] | Highly Flammable |
| D4 | Siloxane | Dry | 1332.2 | 586.5 | 0 | low | Flammable [23] |
| Ethanol | Alcohol | Wet | 6268.7 | 514.7 | -79.8 to 32 [23] | -253 [23] | Severe Flammable |

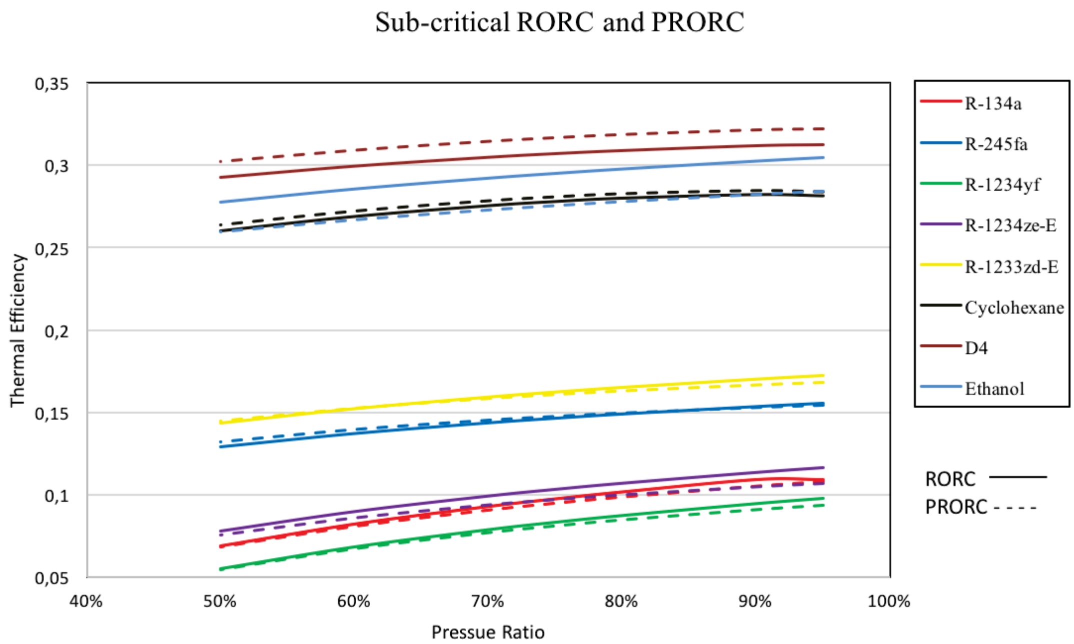


Fig. 1 Sub-critical RORC (solid lines) and PRORC (dashed lines) Thermal Efficiency

TABLE III
EVAPORATOR PRESSURE AND TURBINE INLET TEMPERATURE FOR SUB-CRITICAL CONDITION

| Working Fluid | $P_{eva}$ [kPa] | $T_3 = T_{Turbine,in}$ [K] |
|---|---|---|
| R-134 | 3653.2 | 388.5 |
| R-245fa | 3286.2 | 423.4 |
| R-1234yf | 3043.8 | 374.8 |
| R-1233zd-E | 3213.1 | 436.6 |
| R-1234ze-E | 3271.1 | 389.6 |
| Cyclohexane | 3672.1 | 545.3 |
| D4 | 1198.9 | 579.3 |
| Ethanol | 5641.8 | 600 |

### *B. Thermal Efficiency Analysis*

Fig. 3 illustrates the thermal efficiency outcomes for both configurations with the working fluids. As for the sub-critical RORC, the thermal efficiency results varied between 9,2% and 32,8%. The first working fluid, R-134a was employed as the base line since it has been widely employed for ORC applications. The thermal efficiency obtained of the system was 11%. R-245fa was applied as the second HFC obtaining 15,8% as the thermal efficiency. The temperatures at the inlet of the turbine for R-134a and R-245fa were 388,5 K and 423,3 K respectively. This difference directly influenced the net power output of the system, even though the heat capacities of the two working fluids are akin to each other.

The first HFO application with R-1234yf resulted in 9,2% thermal efficiency, which was the lowest outcome for all RORC. However, the following HFOs, R-1234ze-E and R-1233zd-E, achieved higher thermal efficiencies. As shown in Table II, the critical pressures of the three HFOs are similar values, whereas the critical temperature of R-1233zd-E is fairly higher. Therefore, the application of R-1233zd-E resulted in higher thermal efficiency of 17%. The turbine inlet temperature was 436,6 K for this case. Compared to R-245fa, the critical pressure of R-1233zd-E is lower but the critical temperature is higher. Hence, in terms of operating conditions at lower pressure level and taking into account the environmental side effects, R-1233zd-E could be considered as one of best substitution for R-245fa with better thermal efficiency.

Cyclohexane and D4 are isentropic and dry fluids, in order to satisfy the dry expansion conditions, sub-critical saturated conditions were utilised for both of them. The acquired thermal efficiency for cyclohexane was 29,6%. Compared to the HFC and HFOs applications, the thermal efficiency was considerably higher. This high efficiency value is due to the higher turbine inlet temperature and higher heat capacity of cyclohexane at the engine exhaust temperature. Hence,

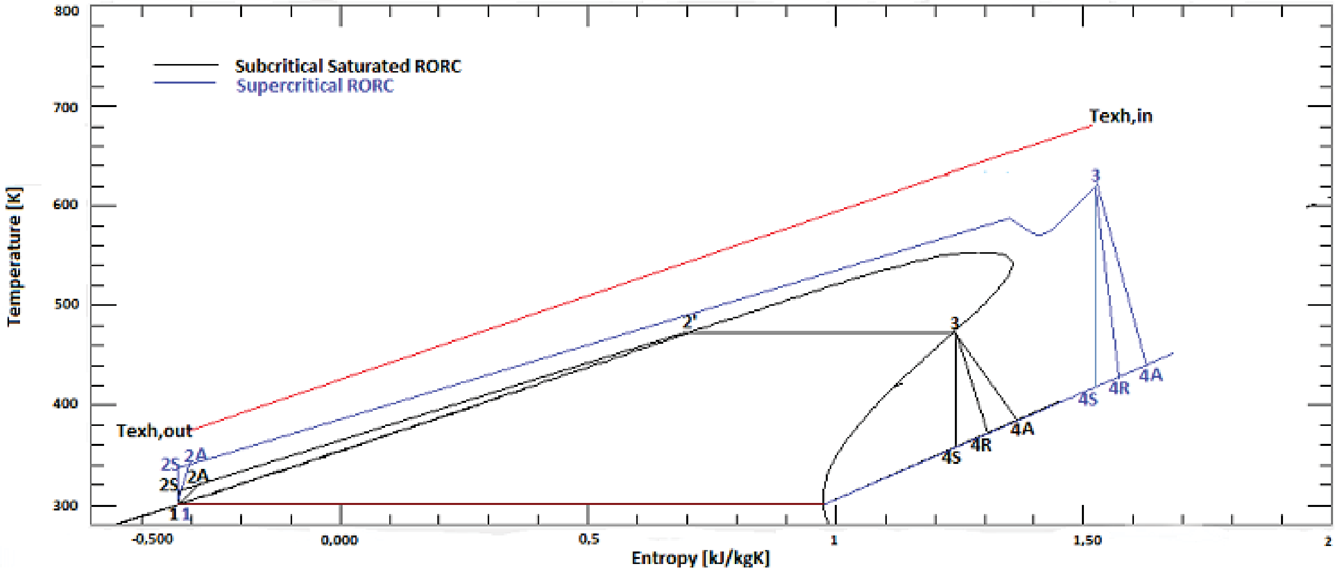


(a) T-s Diagram of Supercritical RORC

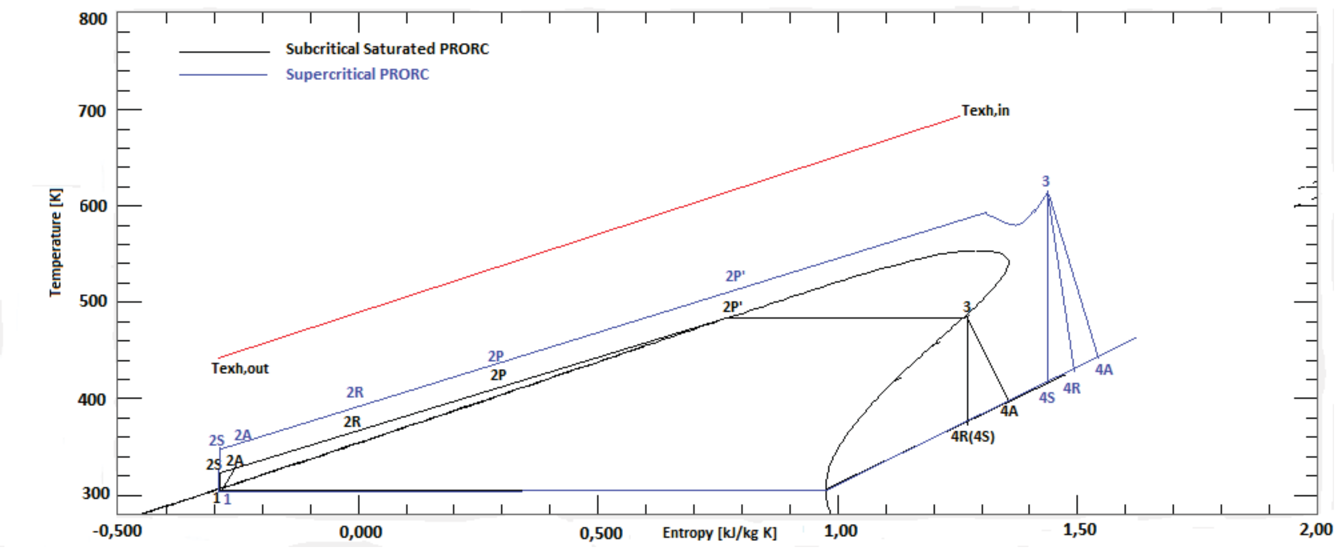


(b) T-s Diagram of Supercritical PRORC

Fig. 2 Supercritical RORC and PRORC Configurations

one of the greatest thermal efficiency of the RORC was obtained with the cyclohexane employment. Similarly, D4 was used as the seventh working fluid for sub-critical RORC and the greatest thermal efficiency of RORC application was procured with a value of 32,8%. Regarding the thermodynamic features, D4 has the lowest critical pressure and highest critical temperature. At the lowest evaporator pressure, the turbine inlet temperature was 579,3 K. In terms of net power output, compared to cyclohexane, D4 employment was slightly lower than cyclohexane, 212 kW and 250 kW respectively, this is due to the lower heat capacity of D4, the difference between the exhaust temperatures at the outlet of the evaporator, where D4 is much higher, is the reason to its highest thermal efficiency.

As the last working fluid, ethanol was applied under the sub-critical superheated RORC conditions. The thermal efficiency outcome of the application was obtained as the second highest due to the high critical temperature. The temperature at the turbine inlet was almost 600 K. Due to its high heat capacity, the maximum amount of heat was extracted from the exhaust, leaving the exhaust gas temperature at the evaporator outlet 371,4 K. Consequently the highest net power output was achieved of 280 kW. The thermal efficiency of D4 was higher than the ethanol application. Table IV summarises the net power outputs for two conditions on RORC configuration.

The same approach was applied for the PRORC configuration with the eight working fluids. The highest and lowest thermal efficiencies were obtained with ethanol and R-1234yf applications with values of 29,2% and 12,2% respectively.

For the HFCs and HFOs, the application of the PRORC showed the same trend as the RORC with respect to thermal

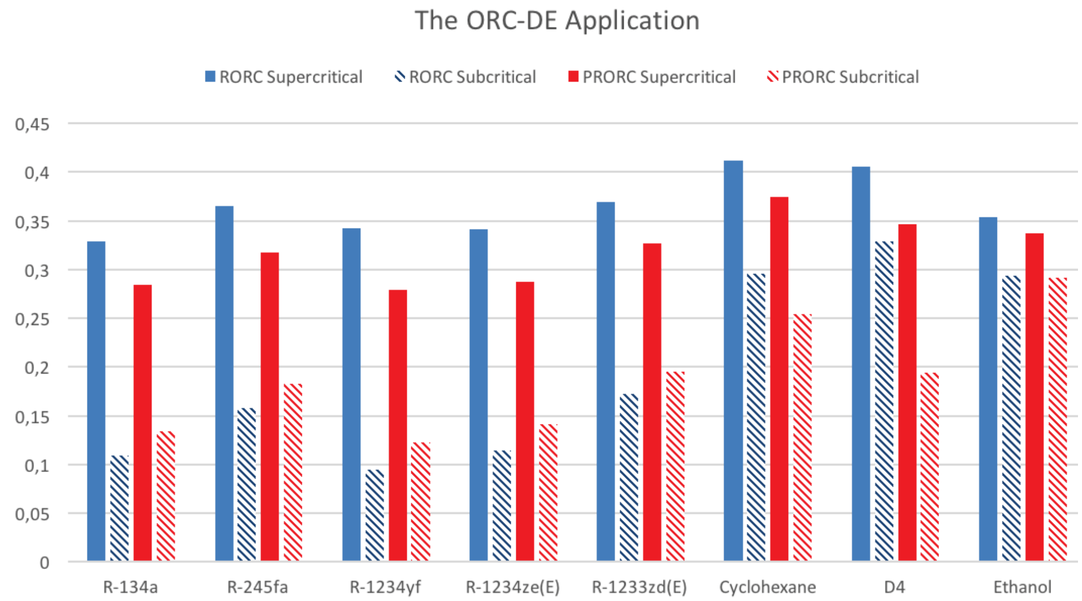

Fig. 3 Thermal efficiency for RORC and PRORC

TABLE IV
RORC POWER OUTPUTS

| Working fluid | $W_{net,supercritical}$ [kW] | $W_{net,sub-critical}$ [kW] |
|---|---|---|
| R-134a | 171,7 | 112,0 |
| R-245fa | 203,1 | 162,2 |
| R-1234yf | 153,3 | 97,3 |
| R-1234ze-E | 175,9 | 118,1 |
| R1233zd-E | 221,1 | 176,1 |
| Cyclohexane | 209,4 | 250,0 |
| D4 | 176,2 | 211,6 |
| Ethanol | 295,8 | 280,3 |

efficiencies. Thus both R-245fa and R-1233zd-E resulted in the highest outcomes of their chemical class with thermal efficiency values of 18,3% and just below 20%. There was an evident increase of thermal efficiency in these five cases (of about 4 points in the percentage value) due to the extra heat subtracted from the water of the cooling system. The thermal efficiency of the cyclohexane application was 25,4% as shown in Fig. 3. The net power output of the systems resulted 209 kW which is slightly lower than for the RORC application. Similarly, for D4 the efficiency and power output for the PRORC were lower than for the RORC efficiency. This was due to the temperature restriction between the pre-heater and engine cooling water. The initial constrain on the PRORC in order to have reasonable heat transfer between the engine cooling water, was setting the inlet and the outlet temperature of the cooling water to 90°$C$ and 80°$C$. Therefore, the working fluid temperature after pre-heating was fixed at 65°$C$ as seen in Fig. 2. Consequently, the temperature at the turbine exit was increased limiting to total power output resulted and lowering the thermal efficiency in comparison to the RORC case.

For the last working fluid, ethanol, the application of PRORC resulted in a slight increase in power output but effectively lower thermal efficiency due to the increase of heat added into the ORC.

Supercritical conditions were applied to both RORC and PRORC configurations with the same working fluids.For supercritical conditions, the evaporator pressure was set to 7 MPa while the temperature was set to 30°$C$ lower (698 K) for the eight refrigerants, than the engine exhaust temperature. Fig. 2 illustrates the T-s diagram for the supercritical application. As expected, the application of supercritical conditions allowed higher turbine inlet temperatures and therefore increasing the thermal efficiency. For HFCs and HFOs, there was an increased of thermal efficiency up to 35% with supercritical condition. The employment of R-134a resulted in 10,8% thermal efficiency with sub-critical condition, whereas 32,8% was obtained for supercritical conditions. Similar trend was observed with the rest of HFC and HFOs. In terms of supercritical conditions, high temperature at the inlet of the turbine was fundamental to high thermal efficiency.

In the RORC, for cyclohexane and D4 the thermal efficiency resulted up to 40% while ethanol was 35%. The thermal efficiency of the cycles was determined by the turbine work and heat transferred to the working fluids, however as the heat capacity of the fluids had a wide range, the total power output differed somehow from the thermal efficiency values, thus Tables IV and V show the total power output obtained with all working fluids. As it can be seen, the maximum power output was achieved for the ethanol case with 295,8 kW representing a total of 22% increase in total power generated, this was due to its high heat capacity and the high inlet turbine temperature.However it is important to notice that for dry fluids like cyclohexane, the application of supercritical condition meant a big increase in Turbine outlet temperature and therefore reducing the power subtracted from the fluid. This was the case for cyclohexane and D4 where total power outputs were much lower than those achieved at sub-critical conditions.

International Science Index, Energy and Power Engineering Vol:12, No:2, 2018 waset.org/Publication/10008559

Supercritical conditions were also used for PRORC set-up with the same procedure. In general, as shown in Table V, the power output achieved was slightly higher than for the RORC, the acquired thermal efficiencies of PRORC were however slightly lower than RORC design's outcomes. The increase in power output was of about 1% for all working fluids, with the exceptions of cyclohexane and D4 for the reasons above mentioned. Therefore the application of PRORC for cases of high temperature waste heat recovery should require a careful analysis since the installation and maintenance cost could counteract the benefits obtained in power output.

TABLE V
PRORC POWER OUTPUT

| Working fluid | $W_{net,supercritical}$ [kW] | $W_{net,sub-critical}$ [kW] |
|---|---|---|
| R-134a | 170,1 | 128,5 |
| R-245fa | 195,8 | 176,2 |
| R-1234yf | 150,8 | 118,0 |
| R-1234ze-E | 173,2 | 135,8 |
| R1233zd-E | 212,1 | 187,7 |
| Cyclohexane | 212,0 | 209,7 |
| D4 | 175,4 | 122,1 |
| Ethanol | 300,5 | 280,9 |

Supercritical applications, as they were expected, resulted in higher thermal efficiency due to the better match between the working fluid and exhaust gases temperature. The greatest thermal efficiency was obtained with cyclohexane application with 41% and D4 with 40%.

### C. Exergy Analysis

RORC and PRORC configurations were evaluated in accordance with the second law thermodynamics. $\eta_{II}$, exergy loss on the exhaust after ORC application and exergy destruction factor of the system (EDF) are the fundamental parameters.

Tables VI and VII depict the second law application outcomes under supercritical and sub-critical conditions on RORC for the eight working fluids. Under supercritical conditions, $\eta_{II}$ results did not vary from each other. The lowest $\eta_{II}$ was acquired with ethanol with 84%. The rest of the working fluids' outcomes were obtained almost same respectively 86%. Deeper analysis on exergy reveals the effect of critical pressure and temperature of the working fluids. $X_{loss}$ after leaving the evaporator values were showed in Table VI. Except for Ethanol, there was a great potential of exhaust gases after RORC application for the seven working fluid. The greatest $X_{loss}$ was obtained with D4 which had the greatest exhaust outlet temperature after the expansion. In supercritical case, exhaust temperature at the exit of turbine is the only leading parameter for $X_{loss}$ of the system due to the fact that the turbine inlet temperature was fixed for all the cases. Furthermore, as the Exergy available was still high after the evaporator, especially, for D4 and R-1234yf could allow the use of more complex systems, such as dual organic rankine cycle.

With regard to high turbine inlet temperature on supercritical conditions, thermal efficiency results are also increased as it is stated in Fig. 3. The increment of thermal efficiency resulted in a reduction of Exergy Destruction.

In terms of sub-critical conditions, in general, $\eta_{II}$ results were slightly lower than supercritical condition due to the lower evaporator pressures and turbine inlet temperatures. With respect to low absolute pressure at the turbine, $W_{net}$ values of the sub-critical condition were lower, therefore , $\eta_{II}$ were as well. The greatest $\eta_{II}$, 86%, was obtained with D4 whereas, the lowest value was obtained with R-1234yf with value of 75%.

The biggest difference between supercritical and sub-critical conditions is the Exergy available in the exhaust after leaving the evaporator. For supercritical case, the lowest exergy available in the exhaust was obtained for ethanol, 49.3 kW, the highest value was 204.7 kW with D4 application. However, under sub-critical conditions, except for D4, the rest of the seven working fluids' outcomes did not exceed 20 kW. Hence, due to the lower evaporator pressure, lower exhaust outlet temperature after turbine and lower exergy available in the exhaust results were found.

With regard to EDF values, the results showed that exergy destructions on sub-critical condition were vaguely higher than the super-critical case. More specifically, HFCs and HFOs resulted with 1.43 to 2.83 EDF, whereas, on supercritical conditions, the values varied around 0.5. Thus, at high turbine inlet temperatures, the energy required to heat up the working fluid increases, meanwhile, the mass flow rate of the working fluid decreases. Consequently, $W_{net}$ of the system decreases. Sub-critical RORC provides lower thermal and the second law efficiencies with lower exergy available in the exhaust after application and higher EDF. Thus, sub-critical conditions could be applied on transportation engines. On the contrary, supercritical RORC results with higher efficiencies with lower mass flow rates and EDFs. Regarding the high exergy in the exhaust after application, more complex cycle such as dual cycle could be proposed.

PRORC application's outcomes are revealed on Tables VIII and IX. The results followed the same trend with RORC application. In terms of $\eta_{II}$, under supercritical conditions, PRORC resulted higher than the sub-critical due to the higher $W_{net}$. $X_{loss,exh}$ values were fairly low in contrast to RORC configuration. The reason why, due to the application of additional heat source, exhaust outlet temperatures were acquired lower. Hence, exergy available in the exhaust after the application outcomes were lower in PRORC case.

Under sub-critical condition, $X_{loss,exh}$ results were calculated equal due to the fixed exhaust outlet temperature after the turbine. However, on cyclohexane and D4 cases, sub-critical saturated conditions were applied. Therefore, higher exhaust outlet temperatures were calculated. Similar to sub-critical RORC application, higher EDF values were acquired with PRORC too.

## IV. CONCLUSION

This paper presented a detailed thermodynamic analysis of waste heat recovery (WHR) with sub-critical and supercritical Organic Rankine Cycle (ORC) application with eight working

TABLE VI
EXERGY OUTPUT ON SUPERCRITICAL RORC

| Working Fluids | $T_{exh,out}$ [K] | $\dot{m}_{workingfluid}$ [kg/s] | $X_{loss,exh}$ [kW] | $\eta_{II}$ [%] | $EDF_{system}$ [%] |
|---|---|---|---|---|---|
| R-134a | 532.4 | 2.16 | 164,3 | 86% | 59% |
| R-245fa | 519.9 | 2 | 149,8 | 86% | 41% |
| R-1234yf | 560.4 | 2.20 | 198,3 | 85% | 56% |
| R-1234ze-E | 534.9 | 2.20 | 167,3 | 86% | 53% |
| R1233zd-E | 504,2 | 2.11 | 132,3 | 86% | 38% |
| Cyclohexane | 537.7 | 0.81 | 170,6 | 86% | 27% |
| D4 | 565.5 | 1.45 | 204,7 | 86% | 32% |
| Ethanol | 415.4 | 0.63 | 49,3 | 84% | 31% |

TABLE VII
EXERGY OUTPUT ON SUB-CRITICAL RORC

| Working Fluids | $T_{exh,out}$ [K] | $\dot{m}_{workingfluid}$ [kg/s] | $X_{loss,exh}$ [kW] | $\eta_{II}$ [%] | $EDF_{system}$ [%] |
|---|---|---|---|---|---|
| R-134a | 342.4 | 5.2 | 8.05 | 76% | 283% |
| R-245fa | 344.6 | 4.5 | 8.8 | 78% | 164% |
| R-1234yf | 341.4 | 6.3 | 7.7 | 75% | 342% |
| R-1234ze-E | 342.3 | 5.4 | 8.1 | 76% | 264% |
| R1233zd-E | 345.8 | 4.4 | 9.3 | 78% | 143% |
| Cyclohexane | 421.2 | 1.5 | 46.8 | 83% | 56% |
| D4 | 486.9 | 2.3 | 113.9 | 86% | 53% |
| Ethanol | 371.4 | 0.77 | 20.8 | 81% | 48% |

TABLE VIII
EXERGY OUTPUT ON SUPERCRITICAL PRORC

| Working Fluids | $T_{exh,out}$ [K] | $\dot{m}_{workingfluid}$ [kg/s] | $X_{loss,exh}$ [kW] | $\eta_{II}$ [%] | $EDF_{system}$ [%] |
|---|---|---|---|---|---|
| R-134a | 503.8 | 2.14 | 126.5 | 86% | 85% |
| R-245fa | 496.9 | 1.92 | 124.4 | 86% | 60% |
| R-1234yf | 525.5 | 2.16 | 156.3 | 85% | 86% |
| R-1234ze-E | 502.6 | 2.17 | 130.6 | 86% | 77% |
| R1233zd-E | 485.2 | 2.02 | 112.2 | 86% | 53% |
| Cyclohexane | 516.3 | 0.82 | 145.7 | 86% | 37% |
| D4 | 538.4 | 1.44 | 171.4 | 86% | 51% |
| Ethanol | 394.5 | 0.64 | 34.5 | 84% | 34% |

TABLE IX
EXERGY OUTPUT ON SUB-CRITICAL PRORC

| Working Fluids | $T_{exh,out}$ [K] | $\dot{m}_{workingfluid}$ [kg/s] | $X_{loss,exh}$ [kW] | $\eta_{II}$ [%] | $EDF_{system}$ [%] |
|---|---|---|---|---|---|
| R-134a | 368 | 5.9 | 19.1 | 76% | 225% |
| R-245fa | 368 | 4.9 | 19.1 | 78% | 137% |
| R-1234yf | 368 | 7.6 | 19.1 | 75% | 254% |
| R-1234ze-E | 368 | 6.2 | 19.1 | 76% | 208% |
| R1233zd-E | 368 | 4.7 | 19.1 | 78% | 123% |
| Cyclohexane | 420 | 1.3 | 51.9 | 83% | 83% |
| D4 | 492 | 3.2 | 119.4 | 86% | 160% |
| Ethanol | 368 | 0.77 | 19.1 | 81% | 49% |



fluids for a stationary diesel engine.The system main parameters of the ORC using different working fluids were optimized with five indicators, $\eta_{thermal}$, $\eta_{II}$, $X_{loss,exhaust}$, $W_{net}$ and EDF namely. The following conclusions can be drawn based on the performance investigation carried out in the present work:

- Under supercritical conditions with RORC configuration, cyclohexane resulted with the highest thermal efficiency. On the other hand, in terms of net power output of the system, ethanol was the best performing working fluid due to its high heat capacity with a value of 296 kW, representing a 22% power increased.
- PRORC set-up showed an increased of power output compared to RORC of about 1% for all working fluids.
- RORC and PRORC sub-critical cycles offered lower thermal efficiency and power output than supercritical cycles, except of the dry and isentropic fluids in, in which the saturated cycle worked in their favour. Thus, for low temperature WHR applications the use of isentropic and dry fluids could be advisable.
- Heavy-duty transportation engines could have their performance improved by 22% with the use of a more economical and light setup using single RORC with ethanol.
- With regard to high exergy available in the exhaust after the Organic Rankine Cycle application with supercritical condition, dual cycle could be suggested to improve the stationary engines' performance approximately 23%.

## Appendix

Pump work,

$$\dot{W}_{pump} = \dot{m}_{wf}.(h_{2a} - h_1) \quad (1)$$

Turbine work,

$$\dot{W}_{turbine} = \dot{m}_{wf}.(h_3 - h_{4a}) \quad (2)$$

The heat transfer rate between the working fluid and the exhaust gas is obtained as follows,

$$\dot{Q}_{in} = \dot{m}_{wf}.(h_3 - h_{2a}) \quad (3)$$

The net work output in the ORC systems,

$$\dot{W}_{net} = \dot{W}_{turbine} - \dot{W}_{pump} \quad (4)$$

Hence, the thermal efficiency of the cycle is calculated,

$$\eta_{cycle} = \frac{\dot{W}_{net}}{\dot{Q}_{in}} \quad (5)$$

n the energy analysis, the mass flow rate of the working fluid is obtained through an energy balance inside the evaporator for both sub-critical and supercritical conditions. The turbine inlet temperature is calculated and fixed for the RORC and PRORC configurations:

$$T_3 = T_{exh,in} - \Delta T_{pp} \quad (6)$$

For the supercritical conditions, as the pinch point approach cannot be applied, the turbine inlet temperature and $T_{min}$ are obtained in accordance with the exhaust gas temperature of the engine.

$$T_3 = T_{exh,in} - T_{pp} \quad (7)$$

$$T_{exh,out} = T_{min} + T_{approach} \quad (8)$$

The working fluid mass flow rate and exhaust outlet temperature are calculated through the pinch point approach for sub-critical ORC applications.

$$\dot{m}_{wf} = \frac{\dot{m}_{exh}.c_{p,exh}.(T_{exh,in} - T_{exh,pp})}{h_3 - h_2'} \quad (9)$$

$$T_{exh,out} = T_{exh,pp} - \frac{(h_2' - h_2).\dot{m}_{wf}}{\dot{m}_{exh}.c_{p,exh}} \quad (10)$$

Following equation (8), if $T_{exh,out} < T_{min}$, a second energy balance is applied in the economizer to find the satisfied mass flow rate of the working fluid for the system.

$$\dot{m}_{wf2} = \frac{\dot{m}_{exh}.c_{p,exh}.(T_{exh,in} - T_{min})}{h_3 - h_{2R}} \quad (11)$$

In the exergy analysis, the dead state is specified as $T_0$ = 25 $^\circ C$ and $P_0$ = 1 atm. The same calculation procedure is applied both sub-critical and supercritical ORCs.

For the pump, the reversible work and the second law efficiency are calculated as follows,

$$\dot{W}_{reversible} = (h_{2a} - h_1) - T_0.(s_2 - s_1) \quad (12)$$

$$\eta_{pump,II} = \frac{\dot{W}_{reversible}}{\dot{W}_{actual}} \quad (13)$$

For the turbine,

$$\dot{W}_{reversible} = (h_3 - h_{4a}) - T_0.(s_3 - s_{4a}) \quad (14)$$

$$\eta_{turbine,II} = \frac{\dot{W}_{actual}}{\dot{W}_{reversible}} \quad (15)$$

The exergy loss through exhaust gases leaving the ORC system is calculated as:

$$X_{loss} = \dot{m}_{exh}.c_{p,exh}.[(T_{exh,out} - T_0) - T_0.log(T_{exh,out}/T_0)] \quad (16)$$

Exergy that is supplied to the system:

$$X_{supplied} = \dot{m}_{exh}.c_{p,exh}.[(T_{exh,in} - T_0) - T_0.log(T_{exh,in}/T_0)] \quad (17)$$

The second law of efficiency of the system is acquired as:

$$\eta_{cycle,II} = \frac{\dot{W}_{net}}{W_{net,rev}} \quad (18)$$

The Exergy destruction factor (EDF) is calculated as:

$$EDF = \frac{E_{destroyed,system}}{W_{net,system}} \quad (19)$$

## References

[1] S. N. Hossain and S. Bari, "Waste heat recovery from the exhaust of a diesel generator using rankine cycle," *Energy Conversion and Management*, vol. 75, pp. 141–151, 2013.
[2] H. Chen, D. Y. Goswami, and E. K. Stefanakos, "A review of thermodynamic cycles and working fluids for the conversion of low-grade heat," *Renewable and sustainable energy reviews*, vol. 14, no. 9, pp. 3059–3067, 2010.
[3] D. A. Arias, T. A. Shedd, and R. K. Jester, "Theoretical analysis of waste heat recovery from an internal combustion engine in a hybrid vehicle," SAE Technical Paper, Tech. Rep., 2006.
[4] A. Uusitalo, J. Honkatukia, T. Turunen-Saaresti, and J. Larjola, "A thermodynamic analysis of waste heat recovery from reciprocating engine power plants by means of organic rankine cycles," *Applied Thermal Engineering*, vol. 70, no. 1, pp. 33–41, 2014.
[5] K. Kulkarni and A. Sood, "Performance analysis of organic rankine cycle (orc) for recovering waste heat from a heavy duty diesel engine," SAE Technical Paper, Tech. Rep., 2015.
[6] C. Sprouse and C. Depcik, "Review of organic rankine cycles for internal combustion engine exhaust waste heat recovery," *Applied thermal engineering*, vol. 51, no. 1, pp. 711–722, 2013.
[7] R. Law, A. Harvey, and D. Reay, "Opportunities for low-grade heat recovery in the uk food processing industry," *Applied thermal engineering*, vol. 53, no. 2, pp. 188–196, 2013.
[8] I. Vaja and A. Gambarotta, "Internal combustion engine (ice) bottoming with organic rankine cycles (orcs)," *Energy*, vol. 35, no. 2, pp. 1084–1093, 2010.
[9] B. Peris, J. Navarro-Esbrí, and F. Molés, "Bottoming organic rankine cycle configurations to increase internal combustion engines power output from cooling water waste heat recovery," *Applied Thermal Engineering*, vol. 61, no. 2, pp. 364–371, 2013.
[10] A. Schuster, S. Karellas, and R. Aumann, "Efficiency optimization potential in supercritical organic rankine cycles," *Energy*, vol. 35, no. 2, pp. 1033–1039, 2010.

[11] S. Glover, R. Douglas, L. Glover, G. McCullough, and S. McKenna, "Automotive waste heat recovery: Working fluid selection and related boundary conditions," *International Journal of Automotive Technology*, vol. 16, no. 3, pp. 399–409, 2015.
[12] R. Freymann, W. Strobl, and A. Obieglo, "The turbosteamer: a system introducing the principle of cogeneration in automotive applications," *MTZ worldwide*, vol. 69, no. 5, pp. 20–27, 2008.
[13] A. F. Agudelo, R. García-Contreras, J. R. Agudelo, and O. Armas, "Potential for exhaust gas energy recovery in a diesel passenger car under european driving cycle," *Applied Energy*, vol. 174, pp. 201–212, 2016.
[14] I. Statistics, "Co2 emissions from fuel combustion-highlights," *IEA, Paris http://www. iea. org/co2highlights/co2highlights. pdf. Cited July*, 2011.
[15] C. Kalra, G. Becquin, J. Jackson, A. L. Laursen, H. Chen, K. Myers, A. Hardy, H. Klockow, and J. Zia, "High-potential working fluids and cycle concepts for next-generation binary organic rankine cycle for enhanced geothermal systems," in *37th Workshop on Geothermal Reservoir Engineering, Stanford, CA, Jan*, 2012.
[16] S. Glover, R. Douglas, M. De Rosa, X. Zhang, and L. Glover, "Simulation of a multiple heat source supercritical orc (organic rankine cycle) for vehicle waste heat recovery," *Energy*, vol. 93, pp. 1568–1580, 2015.
[17] H. Teng, G. Regner, and C. Cowland, "Achieving high engine efficiency for heavy-duty diesel engines by waste heat recovery using supercritical organic-fluid rankine cycle," SAE Technical Paper, Tech. Rep., 2006.
[18] H. Teng, G. Regner, and C. Cowland,, "Waste heat recovery of heavy-duty diesel engines by organic rankine cycle part i: hybrid energy system of diesel and rankine engines," SAE Technical Paper, Tech. Rep., 2007.
[19] "Siemens steam turbine sst-060," http://www.energy.siemens.com/ru/en/fossil-power-generation/steam-turbines/sst-060.htm, accessed: 2002-2017.
[20] E. Wang, H. Zhang, B. Fan, M. Ouyang, Y. Zhao, and Q. Mu, "Study of working fluid selection of organic rankine cycle (orc) for engine waste heat recovery," *Energy*, vol. 36, no. 5, pp. 3406–3418, 2011.
[21] J. Hærvig, K. Sørensen, and T. J. Condra, "Guidelines for optimal selection of working fluid for an organic rankine cycle in relation to waste heat recovery," *Energy*, vol. 96, pp. 592–602, 2016.
[22] H. Tian, L. Chang, Y. Gao, G. Shu, M. Zhao, and N. Yan, "Thermo-economic analysis of zeotropic mixtures based on siloxanes for engine waste heat recovery using a dual-loop organic rankine cycle (dorc)," *Energy Conversion and Management*, vol. 136, pp. 11–26, 2017.
[23] T. Falano, H. K. Jeswani, and A. Azapagic, "Assessing the environmental sustainability of ethanol from integrated biorefineries," *Biotechnology journal*, vol. 9, no. 6, pp. 753–765, 2014.

**Buket Boz** graduated in Environmental Engineering at Istanbul University (Turkey) at 2012. She finished her MSc in Energy Engineering at 2017 from Izmir Institute of Technology (Turkey). Currently, she is a Ph.D. student at DRIMI (Dept. of Mechanical and Industrial Engineering) at the University of Brescia. Her research focus is on modelling Lithium-ion batteries.

**Alvaro Diez** joined the Mechanical Engineering Department at Izmir Institute of Technology (IYTE) in July 2012 as Assistant Professor. His research areas are internal combustion engines, combustion and spray visualization. He has expanded his research interests in combine heat and power and waste heat recovery techniques.